J Supercond Nov Magn (2010) 23: 3–10
DOI 10.1007/s10948-009-0547-9

ORIGINAL PAPER

Ten Years of Spin Hall Effect

G. Vignale

Received: 3 August 2008 / Accepted: 15 June 2009 / Published online: 1 October 2009

Abstract In this short review I survey the theory of the spin Hall effect in doped semiconductors and metals in the light of recent experiments on both kinds of materials. After a brief introduction to different types of spin–orbit coupling in solids, I describe in detail the three conceptually distinct mechanisms that are known to contribute to the spin Hall effect, namely "skew-scattering", "side-jump", and "intrinsic mechanism". The skew-scattering mechanism is shown to be dominant in certain clean two-dimensional semiconductors in which one component of the spin is conserved. In such systems the side-jump mechanism is sub-dominant, but universal in form, and can become dominant if the electron mobility is reduced by changing the temperature. Both skew-scattering and side-jump contributions are generally reduced by spin precession, and skew-scattering is completely suppressed in the linear Rashba model in the absence of magnetic field. Different models of spin–orbit coupling can, however, sustain an intrinsic spin Hall effect. A brief summary of the present experimental situation concludes the review.

Keywords Spintronics · Spin Hall effect · Spin current

1 Introduction

The Spin Hall Effect (SHE) is the generation of a transverse spin current by an electric current, with spin perpendicular to the plane of the two currents [1, 2]. This effect was predicted theoretically by Dyakonov and Perel in 1971 [3, 4]. It is closely related to the Anomalous Hall Effect—the generation of a Hall current in a ferromagnetic material—whose theory had been developed by Luttinger and Karplus [5] and Nozieres and Lewiner [6] back in the 1960s, but differs from it in one essential respect: it does not require magnetic fields and/or ferromagnetism; in other words, it does not require broken time-reversal symmetry.

The theoretical prediction was scarcely noticed until 1999, when Hirsch [7] and later Zhang [8] rediscovered the effect and brought it to the attention of the spintronics community. Since then, there has been plenty of theoretical and experimental activity on the SHE. Theorists have been trying to sort out and clarify the different competing mechanisms of SHE [9–15]. Experimentalists have been able to demonstrate and quantitatively study the spin Hall effect and its inverse (i.e. the generation of a transverse electric current by a spin current) in a variety of systems, including semiconductors like GaAs [16–18] and ZnSe [19] and metals like Al [20] and Pt [21, 22] all the way up to room temperature. The possibility of detecting the SHE by electrical measurements in mesoscopic devices has been theoretically suggested [23]. There has also been a prediction of a qualitatively new effect, the "Quantum spin Hall effect" [24, 25], which is an edge-state effect occurring in material that are insulators in the bulk but nevertheless support quantized spin currents in edge channels (similar to the currents of the quantum Hall effect, but without a magnetic field). This prediction has recently found support in experiment [26].

At the end of the first decade (taking as a starting point Hirsch's 1999 paper) one can say that the SHE its quite well established, even though some uncertainties persist as to the dominant mechanism in some situations. The effect is robust with respect to temperature, and could certainly play a role in the development of spintronics. On the other hand,

G. Vignale (✉)
Department of Physics and Astronomy, University of Missouri, Columbia, MO 65211, USA
e-mail: vignaleg@missouri.edu

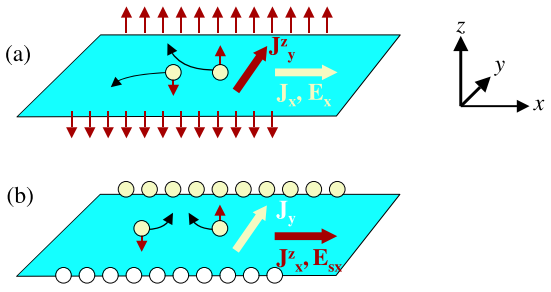

Fig. 1 Spin Hall Effect, direct (**a**) and inverse (**b**)

the initial hopes entertained by many theorists that the effect would prove as universal as the quantum Hall effect have been dashed. It is now clear that the effect is influenced by several different physical mechanisms, which may interfere in unexpected ways, and are strongly dependent on specific material properties. In this review I especially focus on the theory of the SHE in large non-mesoscopic systems, to which the quasi-classical drift–diffusion theory of transport applies.

2 Spin Orbit Interaction

The one thing on which everybody agrees is that the SHE is driven by spin–orbit interactions [27]. Spin–orbit interactions arise from the relativistic theory of the electron–positron system when the positron degrees of freedom are eliminated [28], leaving us to contend with the more familiar two-component spinor wave functions for electrons. The form of the spin–orbit interaction in vacuum is

$$H_{\rm so} = -\frac{\lambda^2}{4\hbar}\left[\mathbf{p}\times\nabla V(\mathbf{r})\right]\cdot\boldsymbol{\sigma} \tag{1}$$

where $\lambda = \frac{\hbar}{mc} \simeq 3.9\times 10^{-3}$ Å is the Compton wavelength of the electron divided by 2π, $V(\mathbf{r})$ is the potential acting on the electron, $\mathbf{p}$ the momentum, and $\boldsymbol{\sigma}$ is the vector of the Pauli matrices. The form of this interaction is traditionally explained as the result of the relativistic transformation of the electric field ∇V to the rest frame of the electron. For our purposes, however, it is better to take a different point of view. Namely, the elimination of the negative energy states from the Dirac equation leads to a redefinition of the original position operator $\mathbf{r}$:

$$\mathbf{r}_{\rm phys} = \mathbf{r} + \frac{\lambda^2}{4\hbar}\mathbf{p}\times\boldsymbol{\sigma}. \tag{2}$$

$\mathbf{r}_{\rm phys}$ is the physical position operator in the positive energy subspace, while $\mathbf{r}$ is the canonical position operator. The replacement of $\mathbf{r}$ by $\mathbf{r}_{\rm phys}$ in $V(\mathbf{r})$, followed by a Taylor expansion to first order in λ, leads immediately to (1). This point of view will play an essential role later in our understanding of the "side-jump" mechanism of SHE. Notice that $\frac{\lambda^2}{4} \simeq 3.7\times 10^{-6}$ Å^2—quite a small value, even on the atomic scale. Nevertheless, spin–orbit effects can be quite significant in atoms and solids, due to the large value of the electric field near the nuclei.

In practice, the fundamental interaction (1) is just the starting point in the construction of an effective spin–orbit hamiltonian for the system under study. In atoms, for example, one arrives at an effective interaction of the form $A_{LS}\mathbf{L}\cdot\mathbf{S}$, where A_{LS} is a constant that depends on the main quantum numbers L and S of the atomic shell, and can be either positive or negative, depending on the occupation of the shell. A similar logic, applied to the solid state, leads to the appearance of an effective interaction of the form

$$H_{{\rm so},n}(\mathbf{k}) = -\frac{1}{2}\mathbf{B}_n(\mathbf{k})\cdot\boldsymbol{\sigma} \tag{3}$$

where $\mathbf{B}_n(\mathbf{k})$ is an effective $\mathbf{k}$-dependent magnetic field that depends on the band index n, just as the coefficient of the $\mathbf{L}\cdot\mathbf{S}$ term in an atom depends on the quantum numbers of the atomic shell. Thus, for example, for the conduction band (c) of zincblende semiconductor GaAs one obtains [27]

$$E_c(\mathbf{k}) = \frac{\hbar^2k^2}{2m^*} + \mathcal{B}\left\{\left(k_y^2 - k_z^2\right)k_x\sigma_x + \ c.p.\right\} + V(\mathbf{r}) + \lambda_c^2\left[\mathbf{k}\times\nabla V(\mathbf{r})\right]\cdot\sigma \tag{4}$$

where $m^* = 0.067m$ is the effective mass of the conduction band, $+\ c.p.$ denotes a sum over cyclic permutations of the indices x, y, z, and $V(\mathbf{r})$ is an external potential distinct from the bulk crystalline potential (e.g. the potential due to impurities). Similar expressions can be derived for the valence bands [29]. The cubic term in this hamiltonian is known as the Dresselhaus term and its magnitude is determined by the constant $\mathcal{B} \simeq 27$ e V Å^3. The last term in the hamiltonian is formally similar to the spin–orbit interaction in vacuum, but its "coupling constant", $\lambda_c^2 \simeq 5$ Å^2, is six orders of magnitude larger. It is quite shocking to realize that the coupling to the external field, while formally similar to the coupling in vacuum, is six orders of magnitude larger and has the opposite sign! Clearly a strong spin–orbit interaction with the nuclei of the periodically arranged atoms (the same interactions that lead to the 0.34 eV gap between the light/heavy hole bands and the split-off valence band of GaAs) is hidden behind the vacuum-like form of this coupling. Equation (4) is the basic model on which our theoretical analysis of the spin Hall effect will be based.

For a GaAs quantum well we must further "project" the Dresselhaus term into the plane of the quantum well. The result of this projection strongly depends on the orientation of the plane. For example, in a [001] quantum well we can set $k_z = \langle k_z\rangle = 0$ and $k_z^2 = \langle k_z^2\rangle = (\pi/d)^2$, where d is the thickness of the quantum well in the z direction. In the limit of

strong confinement ($d \to 0$) this gives the two-dimensional Dresselhaus coupling $H_{001} = \beta\hbar(k_x\sigma_x - k_y\sigma_y)$, where $\beta = -\hbar^{-1}\mathcal{B}(\pi/d)^2$ has the dimensions of a velocity. For a [110] quantum well, we first express the interaction in terms of rotated variables $k_{x'} = k_z$, $k_{y'} = \frac{k_x - k_y}{\sqrt{2}}$, $k_{z'} = \frac{k_x + k_y}{\sqrt{2}}$ and $\sigma_{x'} = \sigma_z$, $\sigma_{y'} = \frac{\sigma_x - \sigma_y}{\sqrt{2}}$, $\sigma_{z'} = \frac{\sigma_x + \sigma_y}{\sqrt{2}}$, where the z' axis is perpendicular to the plane of the quantum well. Then setting $k_{z'} = \langle k_{z'}\rangle = 0$, $k^3_{z'} = \langle k^3_{z'}\rangle = 0$, and $k^2_{z'} = \langle k^2_{z'}\rangle = (\pi/d)^2$ and going to the limit of strong confinement we obtain $H_{110} = (\beta/2)\hbar^{-1}k_{y'}\sigma_{z'}$, which conserves the component of the spin perpendicular to the plane.

In quantum wells it is very convenient to separate the external potential into an in-plane component, due to extrinsic impurities, and a perpendicular component associated with asymmetric confinement. Thus, we write

$$\nabla V = \nabla V_{\text{imp}} + e\mathbf{E}_z, \tag{5}$$

where $\mathbf{E}_z$ is an average electric field perpendicular to the plane.[1] Substituting this in (4) and taking into account the discussion of the previous paragraph we arrive at the following effective hamiltonian for, say, a strongly confined [110] quantum well:

$$E_c(\mathbf{k}) = \frac{\hbar^2 k^2}{2m^*} + \frac{\beta}{2}\hbar k_y\sigma_z - \alpha\hbar(k_x\sigma_y - k_y\sigma_x) + V_{\text{imp}}(\mathbf{r}) + \lambda_c^2\left[\mathbf{k}\times\nabla V_{\text{imp}}(\mathbf{r})\right]\cdot\boldsymbol{\sigma}, \quad ([110]) \tag{6}$$

where $\alpha = e\hbar^{-1}\lambda_c^2 E_z$ is the so-called Rashba coupling constant (the coordinate axes are oriented so that z is perpendicular to the plane of the well).

3 Physical Mechanisms

There are two distinct physical mechanisms of SHE, which differ in the role played by external impurities. The extrinsic mechanism is controlled by the spin–orbit interaction with impurities, e.g. the last term in the hamiltonians (4) or (6). Two specific forms of this mechanism have been identified: (i) the asymmetric scattering (or *skew scattering*) and (ii) the side-jump mechanism. We now describe them in some detail.

Skew scattering—It has long been known that spin-carrying particles are scattered asymmetrically by a central potential in the presence of spin–orbit interaction [30, 31]. In fact, this effect is routinely used to create a spin polarization in an initially unpolarized beam of electrons or neutrons. The situation is particularly simple in two dimensions, for

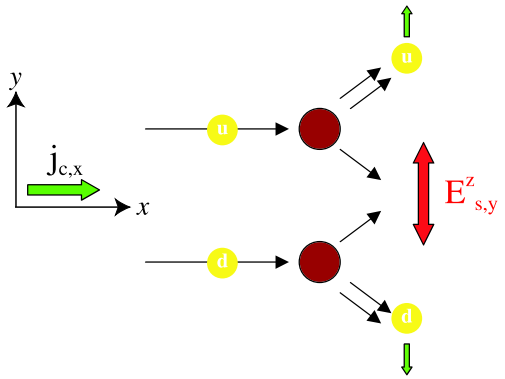

Fig. 2 Semiclassical picture of skew scattering

in this case the spin–orbit interaction with spherically symmetric impurities conserves separately the orbital and the spin angular momentum, L_z and S_z. The scattering cross section depends not only on the scattering angle, but also on the relative sign of L_z and S_z. Thus, a spin-up electron will be more strongly scattered in (say) states of positive L_z than in states of negative L_z, resulting in more electrons being scattered to the left than to the right. The opposite is true for spin-down electrons. The situation is shown schematically in the figure. Of course, the sign of the effect depends on the sign of the potential, i.e. on whether the electron–impurity interaction is attractive or repulsive. It is also worth noting that skew scattering is absent in the Born approximation, and makes its first appearance to third order in the total electron–impurity potential [31].

The simplest way to calculate the contribution of skew scattering to the SHE is to start from a Fermi distribution displaced in the direction x of the electric current j_c, and calculate the rate at which collisions with impurities pump momentum in the transverse direction. The pumping of transverse momentum can be equivalently described as the action of a "spin electric field" $E^z_{s,y}$ (see Fig. 2), which is related to the electric current by a resistivity $\rho_{ss} = \frac{m^*}{ne^2\tau_{ss}}$, where n is the electron density and $1/\tau_{ss}$ the skew scattering rate (we choose this representation of ρ_{ss} because of its obvious resemblance to the ordinary Drude conductivity, but it must be kept in mind that $1/\tau_{ss}$ can have a positive as well as a negative sign depending on the sign of the spin–orbit coupling constant and the electron–impurity interaction). Thus we have

$$E^z_{s,y} = \rho_{ss}\, j_{c,x}. \tag{7}$$

The spin electric field drives a spin current in the y direction according to the linear relation $j^z_{s,y} = \sigma_s E^z_{s,y}$, where σ_s is the spin conductivity. Finally, $j_{c,x}$ is related to the electric field E_x by $j_{c,x} = \sigma_c E_x$ where σ_c is the usual Drude conductivity. Putting all the pieces together we arrive at the

[1] The nature of the "averaging" that determines the value of $\mathbf{E}_z$ is elucidated in [27]. If $\psi_c(z)$ is the wave function of the confined electron, then $\mathbf{E}_z$ is the net field experienced by the *holes*, averaged in $\psi_c(z)$.

following expression for the skew-scattering contribution to the spin Hall conductivity:

$$\sigma_{ss}^{SH} \simeq \sigma_s \rho_{ss} \sigma_c . \tag{8}$$

The skew-scattering rate is calculated straightforwardly from the collision integral of the Boltzmann equation and the asymmetric part of the scattering probability $W^a(\theta)$ [12]:

$$\frac{1}{\tau_{ss}} = \frac{m^*}{4\pi^2\hbar^2} \int_0^{2\pi} d\theta W^a(k_F, \theta) \sin^2\theta, \tag{9}$$

where k_F is the Fermi wave vector. Model calculations presented in Ref. [12] show that $\rho_{ss} \sim 10^{-3}\sigma_c^{-1}$. It should be noted that the asymmetric part of the scattering probability is calculated from standard quantum mechanical scattering theory, without paying attention to the difference between $\mathbf{r}$ and $\mathbf{r}_{\rm phys}$, but rather identifying these two quantities. This is important because the effects associated with the difference between $\mathbf{r}$ and $\mathbf{r}_{\rm phys}$ will be treated separately in the "side-jump" contribution. At the same time, the spin conductivity is given by $\sigma_s = \sigma_c(1+\gamma\tau)^{-1}$, where γ is the spin Coulomb drag coefficient [32–35] and τ the normal momentum relaxation time, which controls the electrical mobility and the Drude conductivity. Thus we arrive at the estimate

$$\sigma_{ss}^{SH} = 10^{-3} \frac{\sigma_c}{1+\gamma\tau}. \tag{10}$$

Notice that the spin Coulomb drag [32–35] reduces the spin Hall conductivity, as expected. However this effect is very significant only in very pure materials $\gamma\tau \gg 1$ and can often be ignored in order-of-magnitude estimates. In 3D semiconductors, with $\sigma_c \simeq 10^3\ (\Omega\cdot\mathrm{m})^{-1}$ we find $\sigma_{ss}^{SH} \simeq 1\ (\Omega\cdot\mathrm{m})^{-1}$ and in 2D semiconductors, with $\sigma_c \simeq 10^{-3}\ \Omega^{-1}$ we find $\sigma_{ss}^{SH} \simeq 10^{-6}\ \Omega^{-1}$. These orders of magnitude are in excellent agreement with experimental findings in n-type GaAs. This and the absence of significant anisotropies suggest that the SHE in these material is most likely of extrinsic origin, and controlled by skew scattering. In 3D metals (Pt), with $\sigma_c \simeq 10^6\ (\Omega\cdot\mathrm{m})^{-1}$ we find $\sigma_{ss}^{SH} \simeq 10^3\ (\Omega\cdot\mathrm{m})^{-1}$, which is about two orders of magnitude smaller than the observed value of $2.4\times10^5(\Omega\cdot\mathrm{m})^{-1}$ [21]. Also in p-type two-dimensional GaAs one experiment [18] reports a value of spin Hall conductivity of the order of $e^2/\hbar \simeq 2\times10^{-4}\ \Omega^{-1}$, significantly larger than the skew-scattering contribution. Both observations have been taken as evidence of an *intrinsic* spin Hall effect. We will return to this point below.

Side-jump—The side-jump is a subtle effect originating from the anomalous form of the velocity operator in spin–orbit coupled systems [6, 36–38]. The physical position operator for the conduction band of zincblende semiconductors is given by (2), with the bare coupling constant λ replaced by λ_c, the coupling constant of the conduction band. Taking the derivative of $\mathbf{r}_{\rm phys}$ with respect to time we get

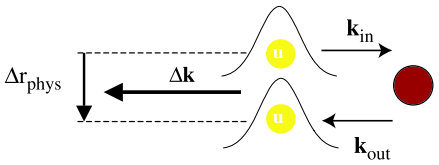

Fig. 3 Semiclassical picture of side-jump in a head-on collision with an impurity. Notice the shift $\Delta\mathbf{r}$ in the trajectory of the back-scattered wave packet

$$\mathbf{v} = \frac{i}{\hbar}\big[\hat{H}, \mathbf{r}_{\rm phys}\big] = \frac{\hbar\mathbf{k}}{m^*} + \frac{2\lambda_c^2}{\hbar}\nabla V_{\rm imp}(\mathbf{r}) \times \boldsymbol{\sigma}\,, \tag{11}$$

where we have neglected terms of second order in λ_c^2. As noted above, the presence of an anomalous velocity is ignored in standard scattering theory, which deals with the scattering of infinitely extended plane waves. Taking into account the anomalous velocity leads to the appearance of additional terms in the Boltzmann equation (or in the Kubo formula) and this is ultimately the origin of the so-called "side-jump" contribution.

The justification for this unusual choice of name lies in a qualitative picture of the electron–impurity collision process, which manages to reproduce the results of more sophisticated calculations without being really discernible in the mathematical treatment. This picture is a semiclassical one: the electron is described not by a plane wave but by a wave packet. Let $\hbar\Delta\mathbf{k}$ be the change in the average momentum of the wave packet in a collision with an impurity. It is evident that this change takes place during the extremely short interval of time during which the wave packet overlaps the impurity. During this short interval of time $\nabla V(\mathbf{r}) = -\hbar\dot{\mathbf{k}}$ is very large and completely dominates the velocity through the second term on the right hand side of (11). Thus, we can disregard the first term and integrating over time we find that the center of the wave packet gets displaced in space by an amount

$$\Delta\mathbf{r}_{\rm phys} = \int dt\ \mathbf{v}(t) = -2\lambda_c^2 \Delta\mathbf{k} \times \boldsymbol{\sigma}\,. \tag{12}$$

This is the "side-jump" effect, depicted schematically in Fig. 3 for the special case of a head-on collision. Notice that the size of the side-jump is *twice* what one would expect naively from (2) and from the change in momentum. The reason for this difference is the change in the internal structure of the wave packet as it scatters off the impurity. This dynamical effect is captured by integrating the velocity over time, but would be missed if we used the static relation (2) between position and momentum.

There are of course all kinds of collisions causing side-jumps in all possible directions but *on the average* an elec-

tron that drifts under the action of an electric field **E** undergoes a momentum change $\Delta\mathbf{k} = e\mathbf{E}$ per unit time—exactly what is needed to balance the pull of the electric field. Substituting this in (12), we see that the average rate of displacement due to the side-jump is at right angles with the electric field. This leads to a net spin current in the y direction, with spin Hall conductivity given by

$$\sigma_{sj}^{SH} = -2\frac{e^2}{\hbar} n\lambda_c^2. \tag{13}$$

The most striking feature of this result is its universality. Although the effect arises from random collisions of electrons with impurities (and possibly with other electrons), the average drift is controlled only by the average rate of momentum transfer, which in turn depends only on the applied electric field. Thus, the side-jump contribution to the spin Hall conductivity of electrons is completely independent of the momentum relaxation time. It is also completely unaffected by electron–electron interactions. Admittedly, this simple result applies only to the s-type conduction bands of zincblende semiconductors. The general theory of the physical position operator and the side-jump effect in more complex bands is developed in Ref. [39] and reviewed in Ref. [40]. This theory defines the position operator in terms of a Berry connection characteristic of the band under consideration. We will restrict our considerations to the simpler electronic problem in what follows.

How does the side-jump contribution compare to the skew-scattering? To answer this, note that

$$\frac{\sigma_{sj}^{SH}}{\sigma_{ss}^{SH}} \simeq 0.3\frac{\lambda_c^2\ [\text{Å}^2]}{\mu\ [\text{cm}^2/\text{V·s}]}\frac{\tau_{ss}}{\tau}\,, \tag{14}$$

where λ_c^2 [Å^2] is the spin–orbit coupling constant expressed in units of Å^2 and μ [cm^2/V·s] is the mobility expressed in units of cm^2/V·s. Making use our previous estimate $\tau/\tau_{ss} \simeq 10^{-3}$ we obtain (in order of magnitude)

$$\frac{\sigma_{sj}^{SH}}{\sigma_{ss}^{SH}} \simeq 3\times 10^2\frac{\lambda_c^2\ [\text{Å}^2]}{\mu\ [\text{cm}^2/\text{V·s}]}. \tag{15}$$

Thus, the relative importance of the side-jump mechanism increases with decreasing mobility. This is expected, since the skew-scattering conductivity is obviously proportional to μ, while the side-jump conductivity is independent of it.[2] At typical semiconductor mobilities ($\mu \sim 10^3$–10^4 cm^2/V·s) we see that the two contributions are of comparable magnitude. Furthermore, one can shift the weight from one to the other mechanism by changing the temperature, which indirectly changes the mobility. This is a particularly interesting exercise in the case of attractive impurities, which is the most common case in n-type semiconductors where the impurities are ionized donors. In this case it can be shown that the skew-scattering conductivity and the side-jump conductivity have opposite signs [12], and the total spin Hall conductivity can be driven through zero by changing the temperature, as shown in Fig. 1 of Ref. [13]. This theoretical prediction has not yet been verified in experiments.

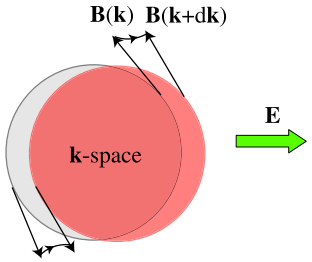

Fig. 4 Schematic picture of intrinsic mechanism of spin Hall effect

Intrinsic mechanism—The last mechanism we want to discuss is called *intrinsic*, because it is associated with the spin-dependent band structure of the material, e.g. with the Dresselhaus term in bulk zincblende semiconductors, or, possibly, with the Rashba term in a two-dimensional GaAs quantum well [10]. The mechanism does not depend explicitly on impurities, yet it would be a serious error to think that impurities can be ignored. Although impurities do not play an "active" role in this mechanism, they are absolutely essential to the establishment of a steady electric current parallel to the electric field (we are considering macroscopic samples in the quasi-classical transport regime). In other words, the spin Hall conductivity must be calculated in the d.c. regime $\omega \ll 1/\tau$, which can be realized only if τ is finite. The essential mechanism of the intrinsic spin Hall effect lies in the precession of the spins about the **k**-dependent magnetic field $\mathbf{B}(\mathbf{k})$ which characterizes the band structure (see (3)). This is qualitatively described in Fig. 3. We start with a steady non-equilibrium state described as a Fermi distribution displaced along the direction of the electric current. By changing the value of **k**, and hence of $\mathbf{B}(\mathbf{k})$ the electric field forces the electrons out of alignment with the effective magnetic field. In the attempt to regain alignment the spins tilt away from the original orientations, and the tilting goes in opposite directions on opposite sides of the Fermi surface. Hence a spin current appears.

In principle, the intrinsic spin Hall conductivity can be calculated from the Kubo formula for the spin-current charge-current response function, without worrying about the spin–orbit coupling to the impurities (normal impurity scattering must however be taken into account as discussed above). In doing this, it is vital to pay attention to vertex corrections, which arise, in general, from averaging over the impurity distribution. In the case of the linear Rashba model

[2] Accordingly, the side-jump contribution to the spin Hall resistivity is proportional to μ^{-2} (square of the Drude resistivity) while the skew-scattering contribution is proportional to μ^{-1}.

inclusion of the vertex correction leads to a vanishing spin Hall conductivity [41–43], in stark contrast with the results of early calculations which did not include the vertex correction [10]. The significance of this surprising result is now well understood, for the spin current in the Rashba model, in the absence of spin–orbit coupling with the impurities, is proportional to the time derivative of a component of the total spin, and such a time derivative must necessarily vanish in the steady state. In some models, however, the vertex correction is either zero or negligible, and when this is the case, an elegant formula (similar to the Streda formula [44] for the quantum Hall conductivity) can be applied. The problem becomes computationally quite complex, but when it is carried out to the end (for example in Pt) [22], it leads to a large spin Hall conductivity, in the range of $10^5\ (\Omega\,\mathrm{m})^{-1}$, which is in quite a good agreement with experiments.

Even in this case, however, it must be noted that the data may be equally well interpretable in terms of extrinsic side-jump effect. For example the observed spin Hall conductivity of Pt, can be interpreted as extrinsic side-jump conductivity if one takes the electron density $n \simeq 6 \times 10^{23}\ \mathrm{cm}^{-3}$ and the coupling constant $\lambda_c^2 = 0.03\ \text{Å}^2$. This value of λ^2 is not unreasonable given the smaller intrinsic length scale of metals (angstroms, rather than hundreds of Angstroms), and actually implies a stronger spin–orbit interaction than in semiconductors, as expected. It is the low mobility of the metallic system ($0.06\ \mathrm{cm}^2/\mathrm{V{\cdot}s}$) that makes the side-jump mechanism so much more important than the skew-scattering mechanisms in this material. So in our view, it is not at all clear that the spin Hall effect in Pt is entirely due to intrinsic spin precession: a significant part of it may be extrinsic side-jump.

Evolution of the spin Hall effect—It should be clear by now that in general the spin Hall effect cannot be ascribed to a single mechanism, but rather several different mechanisms operate simultaneously. Figure 5 shows schematically the evolution of the effect under the naive assumption that different contribution simply add. We describe the evolution in terms of the variable $\hbar\tau/m^*$, which has the dimensions of a squared length and it is therefore suitable for direct comparison with the spin–orbit coupling constant λ_c^2. Furthermore, $\hbar\tau/m^*$ is directly related to the mobility of the system: when expressed in units of Å^2, it turns out to be approximately equal to 6μ, where μ is the mobility in $\mathrm{cm}^2/\mathrm{V{\cdot}s}$. Following Onoda et al. [45] we can define an "ultraclean" regime characterized by the inequality $\frac{\hbar}{\tau} \ll E_{\mathrm{so}}$, where the spin–orbit energy scale E_{so} is given by $E_{\mathrm{so}} = E_F(\frac{\lambda_c}{a})^2 \ll E_F$, where E_F is the Fermi energy and a is the effective Bohr radius. We also have the usual "clean" regime, characterized by the inequalities $E_{\mathrm{so}} \ll \frac{\hbar}{\tau} \ll E_F$, and the "dirty" regime in which $\frac{\hbar}{\tau} > E_F$. In terms of our variable $\hbar\tau/m^*$ these three regimes correspond to (i) $\frac{\hbar\tau}{m^*} \gg \frac{a^4}{\lambda_c^2}$ (ultraclean), (ii) $a^2 \ll \frac{\hbar\tau}{m^*} \ll \frac{a^4}{\lambda_c^2}$ (clean), and (iii) $\frac{\hbar\tau}{m^*} < a^2$ (dirty), where we have assumed $n \sim a^{-3}$. On top of this, we must consider the value of $\hbar\tau/m^*$ below which the side-jump conductivity become larger than the skew-scattering conductivity. According to (15) this happens when $\mu\ [\mathrm{cm}^2/\mathrm{V}\cdot\mathrm{s}] \approx 3 \times 10^2 \lambda_c^2\ [\text{Å}^2]$, which implies $\frac{\hbar\tau}{m^*} \approx 2 \times 10^3 \lambda_c^2$.

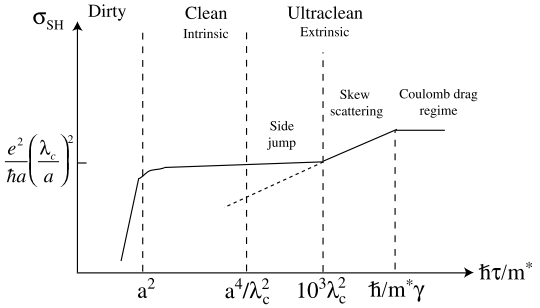

Fig. 5 Possible scenario for the evolution of the SHE as a function of mobility. At high mobility the skew-scattering contribution dominates: it eventually reaches a constant value, to the spin Coulomb drag effect. With decreasing mobility we first enter the side-jump regime, then the intrinsic regime. The crossovers will occur in the inverse order if $a^2/\lambda_c^2 \gtrsim 10^3$

Ironically, the extrinsic skew-scattering effect dominates at very high mobilities. In the absence of Coulomb scattering the spin Hall conductivity would increase in direct proportion to the electrical mobility. It is the spin Coulomb drag that ultimately limits its growth to a value of the order of $10^{-3}\frac{ne^2}{m\gamma}$, where γ is the spin Coulomb drag coefficient.

Decreasing the mobility, one may enter the side-jump regime or the proper intrinsic regime. Which of the two mechanisms sets in first depends on whether $10^3\lambda_c^2$ is larger or smaller than a^4/λ_c^2. In a semiconductor like GaAs, where the effective Bohr radius is about 100 Å, we have $a^4/\lambda_c^2 \simeq 4 \times 10^6 \lambda_c^2 \gg 10^3\lambda_c^2$, so it would be in principle possible to observe a transition from the skew-scattering regime to the intrinsic regime. In a metal like Pt, on the other hand, with $a = 0.5$ Å and $\lambda_c^2 = 0.03\ \text{Å}^2$ we have $a^4/\lambda_c^2 \simeq 70\lambda_c^2 \ll 10^3\lambda_c^2$, so we would expect to see first the transition to the side-jump regime, and then, at lower mobility, the transition to the intrinsic regime. Figure 5 describes the second scenario.

The above considerations are qualitative. In general, we expect that the intrinsic regime and the side-jump-dominated regime will overlap and will be hard to distinguish since they both give σ_{SH} independent of mobility. Furthermore, one must keep in mind the possibility that the spin Hall effect be absent in certain special situations, such as the one described in the next section.

Extended Rashba model—Unfortunately, it is extremely difficult to perform quantitative calculations that take into account all the mechanisms of SHE on equal footing. The only case in which this could be done so far is that of the extended Rashba model for a two-dimensional electron gas,

which includes the following ingredients: (i) linear spin–orbit coupling of the Rashba type (ii) impurity scattering (iii) spin–orbit interaction with impurities (iv) a magnetic field coupling to the spin perpendicular to the plane. The hamiltonian is

$$H = \frac{p^2}{2m^*} + V_{\rm imp}(\mathbf{r}) + \alpha(\mathbf{p}\times\boldsymbol{\sigma})_z + \lambda_c^2\left[\mathbf{k}\times\nabla V_{\rm imp}(\mathbf{r})\right]\cdot\boldsymbol{\sigma} + \hbar\omega_0\frac{\sigma_z}{2}, \quad (16)$$

where $\hbar\omega_0$ is the Zeeman splitting associated with the perpendicular magnetic field.

Unfortunately, this turns out to be a somewhat pathological example, for the reasons explained in Ref. [42] and above. The linear Rashba coupling does not lead to an intrinsic spin Hall effect, and in addition it suppresses (at zero magnetic field) the extrinsic skew-scattering mechanism and substantially reduces the side-jump contribution as shown in Refs. [14, 15]. In this special case the extrinsic d.c. spin Hall conductivity is recovered only by applying an external magnetic field. The fact that the d.c. spin Hall conductivity jumps discontinuously in going from $\alpha = 0$ to a finite value of α, no matter how small, is very surprising. Physically, one would expect a continuous evolution of the static spin Hall conductivity as a function of α. This puzzle has been recently solved by Raimondi and Schwab [46], who have shown the discontinuity to be an artifact of calculations that discard terms of higher order in α, which are responsible for spin relaxation. Thus, the discontinuity of the spin Hall conductivity as a function of α is replaced by an analytic evolution on the scale of $\alpha k_F = 1/\tau_s$, where τ_s is the spin relaxation time [46].

4 Experiments

We conclude with a very brief review of experiments. The first experimental evidence of SHE in semiconductors came from spatially resolved spin polarization measurements in n-type GaAs [16]. In the SHE a charge current induces a transverse spin current, but this spin current cannot flow, due to the presence of boundaries in the y direction. So, unless the spin decays by some relaxation mechanism, a uniform gradient of spin density (spin accumulation) will appear and grow until the spin diffusion current driven by this gradient exactly balances the spin Hall current. In practice, spin relaxation mechanisms cause the spin accumulation to decay exponentially on the scale of the spin diffusion length as one moves away from the geometrical edge of the Hall bar. Nonetheless, the long spin diffusion length of electrons in GaAs allows this spin accumulation to be visualized quite clearly by measuring the Faraday rotation angle of linearly polarized radiation as a function of position across the spin Hall bar. The measured imbalance in the spin chemical potential is of the order of meV s, which translates in a spin Hall conductivity of the order of 1 $(\Omega\cdot\mathrm{m})^{-1}$, consistent with the order of magnitude of the extrinsic mechanism. In another experiment performed in p-type GaAs [18], the spin accumulation was revealed by the polarization of the recombination radiation of holes driven in a two-dimensional LED structure. In this case, the spin accumulation was found to be larger in magnitude and presumably of intrinsic origin. The above experiments were carried out at low temperatures. Observation of SHE at finite temperature has been reported in ZnSe by Stern et al. [19] In spite of the weaker spin–orbit interaction in this material the magnitude of the effect was found to be approximately the same as in low-temperature GaAs. This surprising result suggests that the same factors that weaken the spin–orbit coupling (larger band gap) may also reduce the dielectric screening and thus increase the electron–impurity interaction. More recently, it has become possible to optically inject a charge or spin current [47] and monitor its evolution in real time. This opens the way to the observation of the SHE on shorter time scales than ever before, i.e., in principle, before the establishment of the steady state regime.

Coming to metals, Valenzuela and Tinkham [20] first measured the inverse spin Hall effect in Al. A pure spin current was injected in one arm of an Al cross-shaped device and an electrical potential drop was measured along the other arm. More recently, a similar device has been used to measure both the inverse and the direct spin Hall effect in Pt [21]. The main difference is that there is only a Pt wire, rather than a cross, and the spin current is forced down the thickness of the Pt wire at the junction with paramagnetic Cu. The electric potential induced by the inverse spin Hall effect is measured along the Pt wire.

To sum it the spin Hall effect has been one of the most active and exciting topics of research in condensed matter physics and spintronics in the last ten years. While no form of universality has emerged, it has led to a deeper understanding of spin–orbit interactions in the solid state, and it will likely play an important role in the next generation of spintronic devices, both in metals and semiconductors. It remains a challenge to disentangle experimentally the different physical mechanisms that contribute to the effect.

Acknowledgements This work has been supported by NSF Grant No. DMR-0705460. I thank Ewelina Hankiewicz for a careful reading of the manuscript.

References

1. Engel, H.-A., Rashba, E.I., Halperin, B.I.: Handbook of Magnetism and Advanced Magnetic Materials. Wiley, Chichester (2007)

2. Murakami, S.: Adv. Solid State Phys. **45**, 197 (2005)
3. Dyakonov, M.I., Perel, V.I.: Phys. Lett. A **35**, 459 (1971a)
4. Dyakonov, M.I., Perel, V.I.: Zh. Eksp. Ter. Fiz. **13**, 657 (1971b)
5. Karplus, R., Luttinger, J.M.: Phys. Rev. B **95**, 1154 (1954)
6. Noziéres, P., Lewiner, C.: J. Phys. (Paris) **34**, 901 (1973)
7. Hirsch, J.E.: Phys. Rev. Lett. **83**, 1834 (1999)
8. Zhang, S.: Phys. Rev. Lett. **85**, 393 (2000)
9. Murakami, S., Nagaosa, N., Zhang, S.-C.: Science **301**, 1348 (2003)
10. Sinova, J., Culcer, D., Niu, Q., Sinitsyn, N.A., Jungwirth, T., MacDonald, A.H.: Phys. Rev. Lett. **92**, 126603 (2004)
11. Engel, H.A., Halperin, B.I., Rashba, E.: Phys. Rev. Lett. **95**, 166605 (2005)
12. Hankiewicz, E.M., Vignale, G.: Phys. Rev. B **73**, 115339 (2006)
13. Hankiewicz, E.M., Vignale, G., Flatté, M.: Phys. Rev. Lett. **97**, 266601 (2006)
14. Tse, W.-K., Sarma, S.D.: Phys. Rev. B **75**, 045333 (2007)
15. Hankiewicz, E.M., Vignale, G.: Phys. Rev. Lett. **100**, 026602 (2008)
16. Kato, Y.K., Myers, R.C., Gossard, A.C., Awschalom, D.D.: Science **306**, 1910 (2004)
17. Sih, V., et al.: Nature Phys. **1**, 31 (2005)
18. Wunderlich, J., et al.: Phys. Rev. Lett. **94**, 047204 (2005)
19. Stern, N.P., et al.: Phys. Rev. Lett. **97**, 126603 (2006)
20. Valenzuela, S.O., Tinkham, M.: Nature **442**, 176 (2006)
21. Kimura, T., Otani, Y., Sato, T., Takahashi, S., Maekawa, S.: Phys. Rev. Lett. **98**, 156601 (2007)
22. Tanaka, T., Kontani, H., Naito, M., Naito, T., Hirashima, D.S., Yamada, K., Inoue, J.: Phys. Rev. B **77**, 165117 (2008)
23. Hankiewicz, E.M., Molenkamp, L.W., Jungwirth, T., Sinova, J.: Phys. Rev. B **70**, 241301(R) (2004)
24. Kane, C.L., Mele, E.J.: Phys. Rev. Lett. **95**, 146802 (2005)
25. Bernevig, B.A., Zhang, S.-C.: Phys. Rev. Lett. **96**, 106802 (2006)
26. Koenig, M., Wiedmann, S., Bruene, C., Roth, A., Buhmann, H., Molenkamp, L.W., Qi, X.-L., Zhang, S.-C.: Science **318**, 766 (2007)
27. Winkler, R.: Spin–Orbit Effects in Two-Dimensional Electron and Hole Systems. Springer, Berlin (2003)
28. Foldy, L.L., Wouthuysen, S.A.: Phys. Rev. **78**, 29 (1950)
29. Schliemann, J., Loss, D.: Phys. Rev. B **71**, 085308 (2005)
30. Mott, N.F., Massey, H.S.W.: The Theory of Atomic Collisions. Oxford University Press, London (1964)
31. Landau, L.D., Lifshitz, E.M.: Course of Theoretical Physics, vol. 3. Butterworth-Heinemann, Oxford (1964)
32. D'Amico, I., Vignale, G.: Phys. Rev. B **62**, 4853 (2000)
33. D'Amico, I., Vignale, G.: Europhys. Lett. **55**, 566 (2001)
34. D'Amico, I., Vignale, G.: Phys. Rev. B **65**, 85109 (2002)
35. D'Amico, I., Vignale, G.: Phys. Rev. B **68**, 045307 (2003)
36. Berger, L.: Phys. Rev. B **2**, 4559 (1970) **5**, 1862 (1972)
37. Lyo, S.K., Holstein, T.: Phys. Rev. Lett. **29**, 423 (1972)
38. Crépieux, A., Bruno, P.: Phys. Rev. B **64**, 014416 (2001)
39. Sinitsyn, N.A., Niu, Q., MacDonald, A.H.: Phys. Rev. B **73**, 075318 (2006)
40. Sinitsyn, N.A.: J. Phys. Cond. Matt. **20**, 023201 (2008)
41. Raimondi, R., Schwab, P.: Phys. Rev. B **71**, 033311 (2005)
42. Dimitrova, O.V.: Phys. Rev. B **71**, 245327 (2005)
43. Chalaev, O., Loss, D.: Phys. Rev. B **71**, 245318 (2005)
44. Streda, P.: J. Phys. C **15**, L717 (1982)
45. Onoda, S., Sugimoto, N., Nagaosa, N.: Phys. Rev. Lett. **97**, 126602 (2006)
46. Raimondi, R., Schwab, P.: arXiv:0905.1269v1
47. Zhao, H., et al.: Phys. Rev. Lett. **96**, 246601 (2006)